JOURNAL OF SOLID STATE CHEMISTRY 1, 10–18 (1969)

X-Ray and Low-Temperature Magnetic Studies of the Compounds Hexaammineeuropium (o), Hexaammineytterbium (o), and Their Solid Solutions†

HANS OESTERREICHER,‡ NICHOLAS MAMMANO,‡ AND M. J. SIENKO
The Baker Laboratory of Chemistry, Cornell University, Ithaca, New York 14850

Received December 20, 1968

The compounds $Eu(NH_3)_6$, $Yb(NH_3)_6$, and their solid solutions have been synthesized by direct reaction of the metals with liquid ammonia. Low-temperature X-ray studies at 200K indicate that the unit-cell parameters are very close to those of $Sr(NH_3)_6$, corresponding to a body-centered cubic array of octahedral molecules. A Wigner–Seitz metallic model involving delocalization of electrons through *7s7p* band formation is proposed. Magnetic studies have been carried out by a Faraday method over the range 2.2–300 K and up to 22 kilo-oersted. $Eu(NH_3)_6$ is found to be ferromagnetic with a Curie temperature of 5.5K, which does not change with dilution. Above 5.5K, the paramagnetic moment per europium is 10.15 BM; it changes to 7.9 BM above 47K. As expected, $Yb(NH_3)_6$ is found to be diamagnetic, but it crosses over to paramagnetic below 31K. A model for $Eu(NH_3)_6$ is proposed in which valence electrons, delocalized in a *7s7p* conduction band at higher temperature are progressively frozen out into localized *5d* orbitals below 47K. The extremely large distances over which the ferromagnetic coupling occurs suggests an indirect exchange mechanism via nondegenerate-gas electrons. At higher temperatures, the exchange appears to be of the degenerate-gas type; at very low temperatures, perhaps of the excitonic-insulator type.

Introduction

The rich promise of the metal–ammonia systems as sources of unusual combinations of physical phenomena has been amply fulfilled as modern instrumentation elaborates the detailed behavior of these systems (*1*). The finding that europium can dissolve in liquid ammonia (*2*) adds an important degree of freedom for the systems by allowing insertion of controlled amounts of magnetic-moment carrying ions. The further observation that ytterbium too is soluble in liquid ammonia (*2*) suggests the feasibility of diluting the strongly paramagnetic Eu^{2+} with diamagnetic Yb^{2+} in order to investigate the concentration dependence of magnetic interactions in an electron-rich medium. Warf and Korst in their solubility work surmised that the gold metallic solids formed on evaporation of NH_3 from Eu and Yb solutions were "metal hexammoniates," but these latter were poorly characterized at that time. In the meantime, Holland and Cagle (*3*) have reported that the ammines of calcium, strontium, and barium form body-centered cubic structures with the ammonia molecules arranged octahedrally about the metal atoms in the cell. The actual compositions and cell parameters are found to be variable, and the formula $M(NH_3)_6$ represents only a lower limit for the ammonia content in the absence of solid solution of NH_3 in the compound. The near-identity of the crystal radii of Sr^{2+} (1.10 Å) and Eu^{2+} (1.09 Å) strongly suggests that the space groups and unit-cell parameters might be identical for $Sr(NH_3)_6$ and $Eu(NH_3)_6$.

The first part of this investigation concerned itself with the preparation of $Eu(NH_3)_6$ and with an X-ray study at 200K of the materials prepared. The second part of the study was an examination of the low-temperature magnetic properties of the compounds and some of their solid solutions. The obvious metallic appearance of the compounds, particularly the fact that the coloration is gold and not dull grey as with the no-compound sodium–ammonia system, suggests a delocalized electron model rather like the Wigner–Seitz model recently proposed (*4*) by Mammano and Sienko for $Li(NH_3)_4$. If so, there is a possibility of ferromagnetic coupling of the $4f^7Eu^{2+}$ ions through a Ruderman–Kittel-type

---

† This research was sponsored by the National Science Foundation through NSF grant number GP-6246 and was supported in part by AFOSR 796-67 and ARPA.

‡ Present address: H.O., Oregon Graduate Center, 9340 Barnes Rd., Portland Oregon; N.M., Dept of Chemistry, SUNY at Plattsburgh, N.Y.

interaction via conduction electrons (*5*). To study this, $Yb(NH_3)_6$, which was anticipated to be diamagnetic, was used as a diluent in the mixed system $(Eu, Yb)(NH_3)_6$ to increase the average spacing between the magnetic Eu^{2+} ions.

Experimental

Preparation of Materials. The ammonia was obtained from Matheson and was their highest grade anhydrous 99.99%. The europium was obtained as a 3*N* ingot from Electronic Space Products, Inc. of Los Angeles, and the ytterbium, as a 3*N* ingot from Research Chemicals of Phoenix, Arizona. Metals were transferred in argon-filled glove bags or manipulated in high vacuum distillation chains.

For the X-ray studies, a sliver of metal cut from the ingot was mechanically scraped clean and inserted in an argon-filled, pre-pumped 1-mm capillary. Sodium-dried ammonia was condensed in at 77K and the capillary sealed. On being warmed above 200K, the solid ammonia melted and dissolved the metal. Compositions were controlled by weighing the metals (under argon) and measuring the ammonia pressure drop in a calibrated volume; control was only approximate since samples were too small for high accuracy. Typical weights of metal were 20 mg. For the magnetic studies, specimens were prepared in small bulbs in the same fashion as above. Mixed metal samples were made by placing slivers of europium and of ytterbium in the capillary before NH_3 addition. An attempt was made to have excess ammonia present so that on warming, a completely homogeneous solution would result. Although there was no guarantee that $Eu(NH_3)_6$ and $Yb(NH_3)_6$ did not separately crystallize on cooling, X-ray pictures of $(Eu,Yb)\ (NH_3)_6$ showed only a single phase.

X-ray Data. A conventional Debye camera of 57 mm diameter was modified to allow for flow-gas cooling of the target sample. The metal-ammonia capillary prepared as above was rotated and continually bathed in a cold nitrogen gas stream during the 3–4 hr exposures. A thermocouple adjacent to the sample indicated a temperature of -75 ± 5C. Radiation was CuK_α. The X-ray pictures showed no evidence of any decomposition products such as amide, imide, nitride, oxide, or hydroxide. No lines of ammonia were observed.

Although extreme care was taken to align the samples between the collimators, several of the exposures gave no pattern at all. In such cases, it was surmised that on temperature reduction the sample had moved in the capillary out of the path of the beam, hence suggesting that the compounds are liquid at higher temperatures. To obviate the difficulty, subsequent specimens were mounted so that the beam was not centered at the midpoint of the capillary but at the cooled end. Flow-gas cooling then would reduce the pressure of any residual gases in the capillary and pull the sample into the beam cross-section.

Magnetic Measurements. Magnetic susceptibilities were determined by the Faraday method, using the apparatus and procedure elsewhere described (*6*). Sealed sample bulbs were inserted in a screw-type capsule of copper, which contained the temperature sensors, for suspension in the magnet gap. Force and temperature readouts were compared with calibration curves for the empty capsule. Applied-fields were corrected for internal fields.

Results and Discussion

I. Structure and Energy of Formation

Table I gives representative X-ray data observed for the compounds $Eu(NH_3)_6$ and $Yb(NH_3)_6$. Both patterns index as body-centered cubic with unit cell parameter $a_0 = 9.55$ Å for $Eu(NH_3)_6$ and 9.30 Å for $Yb(NH_3)_6$. These cell parameters are to be compared with those of the corresponding hexammines of the alkaline–earth elements, for which Holland and Cagle (*3*) found $a_0 = 9.12$ Å, 9.57 Å, and 9.97 Å with Ca, Sr, and Ba, respectively. The near equalities in the a_0's of $Eu(NH_3)_6$ and $Sr(NH_3)_6$ and in the a_0's of $Yb(NH_3)_6$ and $Ca(NH_3)_6$ are parallel to corresponding near-equalities in the ionic radii, which, as given by Zachariasen (*7*), are: Eu^{2+} (1.09 Å) and Sr^{2+} (1.10 Å), Yb^{2+} (0.93 Å), and Ca^{2+} (0.94 Å). The agreement, however, might be fortuitous since, according to Holland and Cagle, deviations from stoichiometry are quite probable and can produce significant variations in cell length.

Following the procedure of Holland and Cagle, an intensity analysis was carried out on the X-ray data in terms of a fractional edge parameter u representing positions of the nitrogen atoms on the cell edges. The metal atoms were placed at the body center positions (0,0,0) and $(\frac{1}{2},\frac{1}{2},\frac{1}{2})$ and the nitrogens, at octahedral positions around these—viz, $(u,0,0)$ and $(u+\frac{1}{2},\frac{1}{2},\frac{1}{2})$. Structure factors, and intensities were then calculated for the various diffraction lines. The analysis was somewhat imprecise because the difference in scattering factors of Eu or Yb and N makes the intensity of several of the lines almost independent of choice of u. The best fit was obtained with $u = 0.30 \pm 0.04$ for $Eu(NH_3)_6$ and $u = 0.32 \pm 0.03$ for $Yb(NH_3)_6$. These correspond, respectively,

TABLE I

X-RAY DATA FOR $Eu(NH_3)_6$ AND $Yb(NH_3)_6$

$Eu(NH_3)_6$			$Yb(NH_3)_6$		
2θ	Intensity	(*hkl*)	2θ	Intensity	(*hkl*)
13.40	vs	(110)	13.60	vs	(110)
18.20	m	(200)	18.95	ms	(200)
22.85	m	(211)	23.40	m	(211)
26.10	w	(220)	27.15	w	(220)
29.40	ms	(310)	30.40	m	(310)
32.90	vw	(222)	33.60	vw	(222)
34.95	m	(321)	36.55	mw	(321)
37.50	vw	(400)	38.90	vvw	(400)
40.05	mw	(411), (330)	41.25	vw	(411), (330)
41.90	vw	(420)	43.52	vvw	(420)
44.40	vw	(332)	45.80	vw	(332)
			47.85	vvw	(422)
			50.00	vw	(510)

to an Eu–N distance of 2.9 ± 0.4 Å and a Yb–N distance of 3.0 ± 0.3 as compared to an Sr–N distance of 2.9 ± 0.3 Å.

Although the case for $M\text{–}NH_3$ compound formation appears better documented when M is a divalent metal than when it is a monovalent one (*8*), it was desirable to examine the energetics of the reaction

$$Eu(s) + 6NH_3(l) \rightarrow Eu(NH_3)_6(s)$$

in the same way (*4*) as has been done for $Li(NH_3)_{4(s)}$. As the following analysis shows, the main contribution to stabilization of the compound comes from delocalization of valence electrons due to band formation.

Table II shows the various steps into which the overall reaction can be decomposed and compares the associated free-energy changes for the specific cases of europium, ytterbium, and strontium. (The reference temperature is 25C. No attempt has been made to correct for the difference between free energy and enthalpy in those cases where only enthalpy data were available.) Step I is the sublimation heat for the metals (*9*). Steps II and III correspond respectively to the first and second ionization potentials of the gaseous atoms (*10*).

Step V, the bonding energy of the ion complex in the gas phase, is taken to be the difference in solvation energies between $M^{2+}(g)$ and $M(NH_3)_6^{2+}(g)$.

TABLE II

ENERGY CONTRIBUTIONS TO $M(NH_3)_6$ FORMATION (IN eV)

	Process	M = Eu	M = Yb	M = Sr
I	$M_{(s)} \rightarrow M_{(g)}$	1.87	1.86	1.69
II	$M_{(g)} \rightarrow M^{+}_{(g)} + e^-$	5.73	6.25	5.69
III	$M^{+}_{(g)} \rightarrow M^{2+}_{(g)} + e^-$	11.30	12.10	10.98
IV	$6NH_{3(l)} \rightarrow 6NH_{3(g)}$	+1.82	1.82	1.82
V	$M^{2+}_{(g)} + 6(NH_3)_{(g)} \rightarrow M(NH_3)^{2+}_{6(g)}$	−9.5	−10.1	−8.9
VI	$M(NH_3)^{2+}_{6(g)} + 2e^- \rightarrow M(NH_3)_{6(g)}$	−8.02	−8.15	−7.15
VII	$M(NH_3)_{6(g)} \rightarrow M(NH_3)_{6(\text{molec solid})}$	−0.94	−1.02	−0.51
VIII	$M(NH_3)_{6(\text{molec})} \rightarrow M(NH_3)_{6(\text{metal})}$	−4.04	−4.13	−4.04
Net	$M_{(s)} + 6NH_{3(l)} \rightarrow M(NH_3)_{6(s)}$	−1.78	−1.28	−0.42

The former is determined from experimental data in a manner completely analogous to that used for the $Li(NH_3)_4$ case (*4*), assuming that the heats of solution of Eu and Yb metals are the same as for Sr metal, and that this value is the standard heat of solution (−0.9 eV). The heats of solution of Ca, Sr, and Ba are close to each other, and it is reasonable to assume that the Eu and Yb solution heats are comparable. The solvation energy of $M(NH_3)_6^{2+}(g)$ is calculated from the Born equation applied to a divalent ion in liquid ammonia. The radii of $Eu(NH_3)_6^{2+}$ (3.4 Å) and $Yb(NH_3)_6^{2+}$ (3.5 Å) are determined from the X-ray results; the Latimer cation-radius correction in liquid ammonia appears to be 0.56 Å. Step V was also computed as a summation of ion-dipole interactions following the method used by Coulter (*11*). For Yb, the result was the same as shown in the table; for Eu and Sr, the result was −11.2 instead of −9.5 and −8.9 eV, respectively. The net effect of the alternate calculation would have been to make the compounds even more stable than shown for the net change in Table II.

Step VI, in which two electrons are added in the gas phase to the ion complex, is calculated as the sum of a 7*s* orbital energy, a 7*p* orbital energy, and a correction term for the Coulombic attraction between a positive ion and an electron. The correction term is needed because the 7*s* and 7*p* orbital energies give only the energy involved in ionizing a neutral species, whereas the recapture of the 7*s* electron is by a 2+ ion and the recapture of the 7*p* electron is by a 1+ ion. Standard tables were used for the 7*s* and 7*p* energies (*12*). The justification for assigning one electron capture each to the 7*s* and 7*p* levels, rather than both electrons to the 6*s* or 7*s*, is that the 6*s* orbital is not available (having been pre-empted for d^2sp^3 bonding of the NH_3) and a doubly occupied 7*s* orbital would lead to difficulty later when band formation from overlap of only $7s^2$ would yield an insulator.

Step VII is visualized as the condensation of neutral $M(NH_3)_6$ molecules to a *molecular* solid—i.e., one in which band formation has not yet occurred but outer electrons are in localized 7*s* and 7*p* orbitals. To estimate the energy for this molecular condensation, per-gram values have been averaged for several symmetrical hydrocarbons of roughly equivalent molar mass and then the per-gram values have been converted to molar values by multiplying with the molar mass of the appropriate $M(NH_3)_6$ species.

Step VIII corresponds to the energy change associated with conversion of the molecular solid to a metal—i.e., delocalization of the outer electrons through conduction-band formation. As was done (*4*) for $Li(NH_3)_{4(s)}$, the delocalization energy was taken to be $[(-1.80/r_s) + (2.21/r_s^2)]$ Ry, where r_s, in units of Bohr radii, is the radius of the equivalent Wigner–Seitz sphere (*13*). The correlation energy is $-0.115 + 0.031 \log r_s$. In the body-centered cubic structure of $M(NH_3)_6$, there are two molecules per unit cell, each of which contributes two electrons to the conduction band. Hence, there are four electrons, or four Wigner–Seitz spheres, per crystallographic unit cell. For $Eu(NH_3)_6$, $Yb(NH_3)_6$, and $Sr(NH_3)_6$, the Wigner–Seitz radii come out to be $7.15a_0$, 6.88_0, and $7.15a_0$, respectively. (It is interesting to note that an almost identical value, $7.25a_0$, was obtained for $Li(NH_3)_4$, thus underlining the importance of electron volume in fixing the structure dimensions).

As can be seen from the table, the energies for Steps I–VII just about cancel each other. Still the net process comes out to be energetically favorable, because of the large negative contribution of the Wigner–Seitz delocalization energy. (The same situation was found for $Li(NH_3)_4$.) Detailed comparison of the individual figures is not warranted because of the approximate nature of many of the terms and because of the relatively large uncertainty in the critically important M–N distance. However, one can make the qualitative observation that $Yb(NH_3)_6$ appears to be less stable than $Eu(NH_3)_6$, partly because of the larger ionization potentials of Yb (Steps II and III) and partly because of the weaker binding energy between Yb^{2+} and NH_3 (Step V). The former difference is certainly significant and stems from the imperfect screening of 6*s* orbitals by 4*f* electrons; the latter is subject to doubt because of the previously mentioned uncertainty in the *u* parameter. Given that Eu^{2+} is larger than Yb^{2+} one would expect *a priori* the bond energy of Eu^{2+}–NH_3 to be less than that of Yb^{2+}–NH_3.

The lower stabilization energy for $Sr(NH_3)_6$ is attributable to its lower molecular mass and to a lower bond energy for Sr^{2+}-to-NH_3. The lower stabilization energy is in qualitative agreement with the observed fact that $Sr(NH_3)_6$ (s) appears not to be a very stable system and decomposes most readily of the three.

II. Magnetic Properties

$Eu(NH_3)_6$. There are two extraordinary features seen in the magnetic behavior. One is the decided increase in magnetic moment below 47K, and the other is the appearance of ferromagnetic behavior in the liquid helium range. Figures 1 and 2 show the course of the reciprocal molar susceptibility vs.

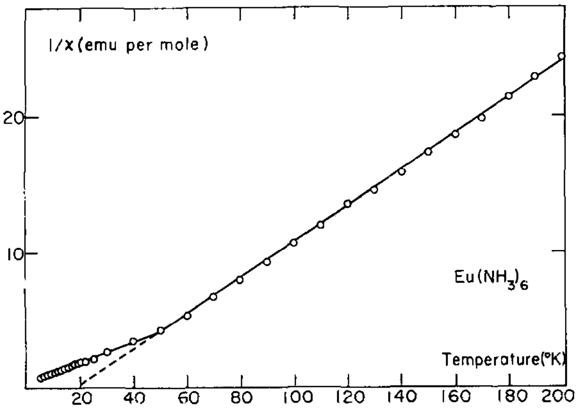

FIG. 1. Reciprocal molar susceptibility (χ_m^{-1}) vs. temperature for Eu(NH$_3$)$_6$.

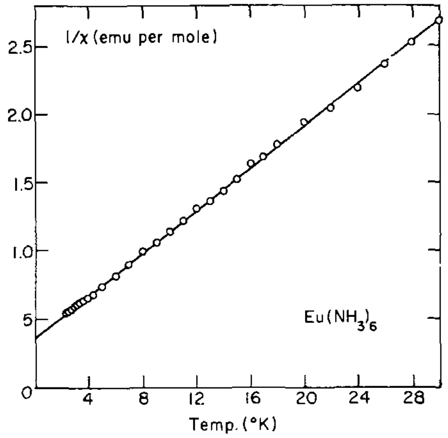

FIG. 2. Low-temperature behavior of reciprocal molar susceptibility (χ_m^{-1}) vs. temperature for Eu(NH$_3$)$_6$.

temperature for a typical specimen of Eu(NH$_3$)$_6$. The data are fitted by two linear dependences of the Curie–Weiss type $\chi = C/(T\text{-}\theta)$, with a change from one dependence to the other at about 47K. Evaluation of the Curie constants C, from the slope of the χ^{-1} vs. T plot, leads to an effective moment of 7.9 BM above 47K and 10.15 BM below 47K, using the defining relation $\mu_{\text{eff}} = 2.83C^{1/2}$. The Weiss constants θ, obtained from the extrapolated intercepts of the χ^{-1} vs. T plots, are +18° for the temperature region above 47K and −5°, below 47K. In the absence of crystal-field effects leading to temperature-dependent moments, a positive θ is generally taken to be indication of ferromagnetic exchange interaction and a negative θ, antiferromagnetic ones. In the case of Eu(NH$_3$)$_6$, some kind of magnetic ordering had actually been expected, probably in a weak form because, although the Eu^{2+} core moment is very great (7.9 BM, $4f^7$ configuration), the separation between cores is also very great (8.27 Å). Hence, the finding of a small ferromagnetic Weiss constant was gratifying. However, it had not been anticipated that the effective moment would rise at lower temperature. The rise might be explained in a novel but reasonable way taking into account the unusual properties of Eu(NH$_3$)$_6$. It is a metal at higher temperature and the model presented in Part I envisions the conduction electrons to be $7s7p$ electrons of the europium, probably far enough from the nucleus that, as in the case of metallic Li(NH$_3$)$_4$, the electrons are substantially on the outside of the ammonia cage that surrounds the central ion. Thus, Eu(NH$_3$)$_6$ can be regarded as a $4f^7$ Eu^{2+} ion in an ammonia cage surrounded by a sheath of electrons which overlaps other similar sheaths. Since the metallic electrons are practically all spin-paired as a Fermi gas, only the $4f^7$ electrons show up in the magnetic moment. In the ground state of $4f^7$, we have $L = 0$, $S = 7/2$, $J = 7/2$, $g = 2$, and $\mu_J = g[J(J+1)]^{1/2} = 7.94$ BM in good agreement with the observed high-temperature moment. We now postulate that on lowering the temperature below 47K, electrons begin to be frozen out of the $7s7p$ conduction band into localized states, either $4f$- or $5d$ states on the europium. If the conduction electrons were completely frozen out, there would be two more electrons localized on each europium, giving either $4f^9$ or $4f^7\ 5d^2$. The $4f^9$ configuration for which $L = 5$, $S = 5/2$, $g = 1.33$, and $\mu = 10.63$ BM, is less likely because of the greater interelectronic repulsion. For the $4f^7\ 5d^2$ configuration, the moment could range from 6.2 to 12.8 BM, depending on the type of coupling assumed. Making the assumption that the orbital moment in the $5d$ orbitals is small and that the spin moments of the $4f$ and $5d$ electrons are strongly coupled, we find the most probable moment for the $4f^7\ 5d^2$ configuration to be 10.0 BM. Thus, no matter which configuration is selected, it appears that the observed low-temperature moment of 10.2 BM can be rationalized. From the data of Fig. 1, it is not possible to decide unequivocally that the change from 7.9 to 10.2 BM occurs discontinuously at 47K. It may be spread over a considerable temperature range, corresponding to gradual withdrawal of electrons from a conduction band or to the gradual splitting off of localized states from a main band. On the other hand, it may be abrupt, in which case a simultaneous change in crystallographic symmetry and electrical conductivity might be expected. (Further studies on these and other properties are now in progress.) Figure 2 presents the low-temperature data for Eu(NH$_3$)$_6$ in greater detail.

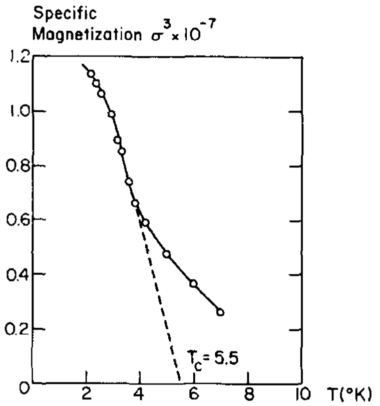

FIG. 3. Third power of specific magnetization (σ^3) at 18,000 Oe vs. temperature for $Eu(NH_3)_6$.

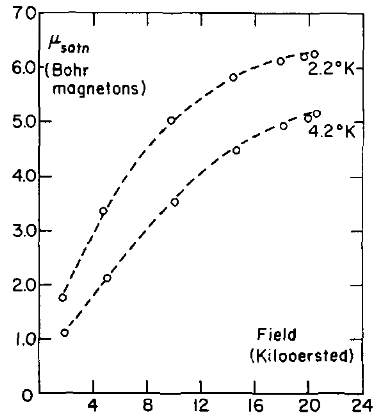

FIG. 4. Magnetic moment, μ as a function of magnetic field in the ferromagnetic region for $Eu(NH_3)_6$.

The consistent linearity of the χ^{-1} vs. T plot shows that the effective moment remains remarkably constant in the 4–30K range. There is, however, a small but significant deviation around 4K, resulting from spontaneous ordering below the Curie temperature, which appears to be at 5.5K. Studies of the susceptibility at 4.2K showed that it is field-dependent.

There are several ways to determine the Curie temperature (*14*). One is to plot the magnetization at a fixed field strength as a function of temperature and observe the point of inflection in the curve. This is the least precise method and, for $Eu(NH_3)_6$, leads to a Curie temperature of 3.3K. A second method is to plot the square of the magnetization vs. temperature and extrapolate the assumed parabolic dependence to zero magnetization in the fixed field. For $Eu(NH_3)_6$, this method gives 7.2K. A third method, for which the theoretical justification appears the most sound, is to plot the third power of the magnetization vs. temperature and extrapolate to zero magnetization. For $Eu(NH_3)_6$, this method as shown in Fig. 3, gives 5.5K, which is taken to be the most probable value of T_c. (A fourth method was also tried in which a $\chi^{-3/4}$ vs. T plot was extrapolated to give $T_c = -13$K. It is believed that the fields used were too high and additional interactions as mentioned below were present so as to negate the applicability of this method).

In the ferromagnetic region, attempts were made to determine the saturation moment of $Eu(NH_3)_6$. Figure 4 shows how the magnetic moment (determined from the observed magnetization) changes with field strength at 4.2K and also at 2.2K. Even at the highest fields used, 20,600 Oe, it is evident that the moments are not yet saturated. From extrapolations to zero reciprocal field of μ vs. $1/H$ curves, it appears that the true saturation moment could be 7.00 BM at 4.2K and 7.31 BM at 2.2K. For seven unpaired spins as in a simple Eu^{2+} core, the expected saturation moment is 7.00 BM; for nine spins as in $4f^7\ 5d^2$ configurations, 9.00 BM. If the $4f^7\ 5d^2$ model mentioned above is correct, it may be that the observed saturation moment is lower than expected because of canting of spins or because of the appearance of another interaction, perhaps antiferromagnetic, at very low temperatures. We already have a hint of this in Fig. 2 where the Weiss constant for the low-temperature segment is negative.

$Eu_xM_{1-x}(NH_3)_6$. In order to understand better the nature of the ordering exchange interactions between the europium atoms, attempts were made to prepare diluted systems in which diamagnetic Yb^{2+} or Sr^{2+} replaced a fraction of the Eu^{2+} ions and, hence, increased the average spacing between the magnetic moments. As indicated below, $Yb(NH_3)_6$ and $Sr(NH_3)_6$ are not straightforward diamagnetic diluents at very low temperatures, being subject apparently to their own conduction band perturbation, but their magnetic moments were low enough to make the experiment interesting. Figure 5 shows some of the results as plots of reciprocal molar susceptibility vs. temperature for three specimens differing in europium content.

In all three cases, Curie–Weiss linear dependences are appropriate at low temperatures. At high temperatures, this also appears true for $Eu_{0.36}Yb_{0.64}$ and $Eu_{0.26}Sr_{0.74}$, but the curve for $Eu_{0.085}Yb_{0.915}$ shows decided curvature over the whole temperature range above 75K. The other noteworthy feature of Fig. 5 is that the change from low- to high-temperature segments does not appear to be as abrupt as in

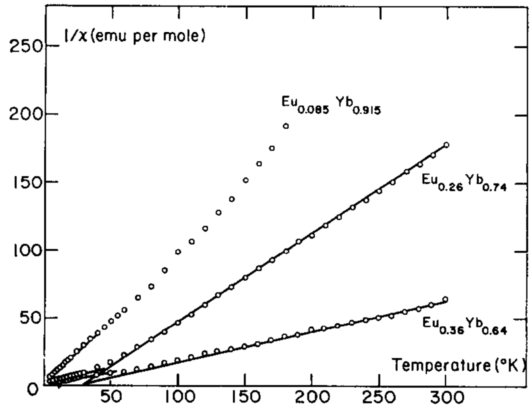

FIG. 5. Reciprocal molar susceptibility (χ_M^{-1}) vs. temperature for $Eu_{0.36}Yb_{0.64}(NH_3)_6$, $Eu_{0.26}Yb_{0.74}(NH_3)_6$, and $Eu_{0.085}Yb_{0.915}(NH_3)_6$.

Fig. 1. Table III collects the magnetic parameters for the diluted systems and compares them with those for $Eu(NH_3)_6$. The values quoted are for 1 mole of complex $M(NH_3)_6$. Because the forces were so large, no corrections have been applied for the diamagnetism. If it is assumed that the Yb or Sr do not contribute to the moment, then the observed molar susceptibility can be attributed to the europium atoms alone. The parenthetic values shown in Table III are those calculated on this basis. (For μ_{eff}, it is necessary to divide by the square root of the europium concentration, since the moments are not additive but the susceptibilities are, at least in the paramagnetic region. For μ_s, one simply divides by the europium concentration, moments being additive in the ferromagnetic region.) Because of the imprecision in determining the europium masses, there is appreciable uncertainty in the computed values. For example, a 10% uncertainty in measuring the europium content can easily lead to an uncertainty of 0.5 BM in the effective moment. The error may be considerably larger than this for $Eu_{0.085}Yb_{0.915}$.

As can be seen from a comparison of the values of Table III, the Weiss constants do not show much change in dilution, the high-temperature one, θ_2, being shifted somewhat to higher values and the low-temperature one, θ_1, being essentially unchanged. There appears to be a slight trend of increasing θ_2 with decreasing europium content, but it may not be significant. The fact that θ_2 does *not* diminish with dilution is very significant since it indicates that the Weiss ferromagnetic interaction in the high-temperature regime is not critically

TABLE III

MAGNETIC PARAMETERS FOR $M(NH_3)_6$

Composition[a]	Weiss constant θ	Effective moment[f] μ_{eff}	Curie temp T_c	Saturation moment[f] μ_s
$Eu(NH_3)_6$	+18°[b]	7.90	5.5°	7.00[d]
	−5°[c]	10.15		7.31[e]
$Eu_{0.36}Yb_{0.64}(NH_3)_6$	+24[b]	4.04(6.7)	5.5	2.58(7.1)
	−5°[c]	6.46(10.7)		
$Eu_{0.26}Sr_{0.74}(NH_3)_6$	+29[b]	3.76(7.3)	6.1	1.78(6.8)
	−6[c]	5.67(11.1)		
$Eu_{0.085}Yb_{0.915}(NH_3)_6$	+30[b]	3.05(10.4)	6.1	0.74(8.7)
	−3[c]	3.21(11.1)		
$Yb(NH_3)_6$	$\chi_m = 7.55 \times 10^{-3}$ at 4.2K; $\mu_{eff} = 0.50$ BM crosses over to diamagnetic above 31K			
$Sr(NH_3)_6$	$\chi_m = 8.2 \times 10^{-3}$ at 4.2K; $\mu_{eff} = 0.53$ BM crosses over to diamagnetic above 22K			

[a] All preparations contained from 3 to 10% ammonia in excess of 6:1 stoichiometry.
[b] Above 47K.
[c] Below 47K.
[d] At 4.2K.
[e] At 2.2K.
[f] Parenthetic values are calculated per mole of Eu.

dependent on increasing inter-europium spacing. Because of this and because the distance over which interaction occurs is very large, going from 8.27 Å in $Eu(NH_3)_6$ to 18.8 Å in $Eu_{0.085}Yb_{0.915}(NH_3)_6$, it is believed that the interaction proceeds through the conduction-band electrons, perhaps as in the Ruderman–Kittel indirect exchange model (*5*). However, the independence of θ of dilution is unexpected since the Ruderman–Kittel model predicts oscillations in the sign and magnitude of θ with increasing interatomic spacing.

The second noteworthy feature of Table III is that the effective moment *per europium* stays approximately constant at 10.7–11.1 BM in the low-temperature region but varies from 6.7 to 10.4 BM in the high-temperature region. In the high-temperature region the drop from 7.90 BM in $Eu(NH_3)_6$ to 7.3 BM in $Eu_{0.26}Sr_{0.74}(NH_3)_6$ is not considered significant, but the 10.4 BM value for

$$Eu_{0.085}Yb_{0.915}(NH_3)_6$$

is probably real. It cannot be explained by error in stoichiometry control, given the good correspondence in the low-temperature range. It may be that with very low contents of europium, the behavior of the system $M(NH_3)_6$ is no longer dominated by the europium moments. Alternatively, it may be, as suggested from Fig. 5, that the kink from low-temperature behavior to high-temperature behavior can occur only if a critical europium content is reached.

The third feature of Table III that needs to be remarked is that the Curie temperature T_c changes little if any with dilution. One possible explanation is that Eu is crystallizing separately as a distinct $Eu(NH_3)_6$. The X-ray data, however, as mentioned before, showed only a single phase. Furthermore, segregated crystallization of $Eu(NH_3)_6$ would make difficult a consistent picture for the unusual behavior of $Eu_{0.085}Yb_{0.915}(NH_3)_6$. A more likely explanation is that the exchange interaction in the ferromagnetic region is indeed independent of inter-europium distance. Such would be the case, for example, if the indirect exchange were not of the Ruderman–Kittel type but of the type found by Baltensperger and de Graaf (*15*) for a nondegenerate electron gas. Whereas the Ruderman–Kittel interaction is for a degenerate electron gas and relatively strong for short ranges but oscillating from ferromagnetic to antiferromagnetic depending on the polarization oscillation, the Baltensperger–de Graaf interaction is a weaker one that remains always ferromagnetic even though it extends over long distances. The mechanism of the latter coupling is through Boltzmann electrons, such as might exist in a semi-conductor with only a few of the electrons excited to the conduction band. In our model of $Eu(NH_3)_6$, it is postulated that the conduction electrons are frozen out to localized states below 47K. If, however, a small fraction remain thermally excited in the conduction band, we might have the conditions required for the Baltensperger–de Graaf interaction. A study of the electrical resistivity behavior in the neighborhood of the 47K-transition would be useful in helping to define the correct model. A rise in resistivity below 47K would be taken as supporting evidence for a change in exchange interaction from Ruderman–Kittel to Baltensperger–de Graaf types. The fact that the energy associated with the Curie Temperature (5.5K) is less than that associated with the Weiss temperature (18–30K) would be in line with the expectation that the Boltzmann-electron interaction is weaker than the Fermi-electron interaction.

The final point to be remarked from Table III is that the saturation moment per europium atom is apparently independent of europium concentration, except perhaps for the most dilute sample $Eu_{0.085}Yb_{0.915}(NH_3)_6$. As noted, below, the behavior of $Yb(NH_3)_6$ at very low temperature suggests it is not a simple diamagnetic material as might be predicted, since it appears to develop an appreciable moment of its own in the liquid helium region. It may be that in the ferromagnetic region the europium is not alone in contributing to the saturation moment.

It might also be noted that all four of the europium-containing preparations shown in Table III showed a negative Weiss constant for the low-temperature portion of the χ^{-1} vs. T curves. This suggests that at very low temperatures, a third interaction might be setting in. It would have to be antiferromagnetic and extremely weak. If, as expected, the $M(NH_3)_6$ systems go insulating at very low temperatures, a possible candidate for this interaction would be virtual excitations from the valence band as postulated by Bloembergen and Rowland (*16*). Given the rich diversity of the phenomena found in metal–ammonia systems, it would only be fitting to find that the $M(NH_3)_6$ systems indeed represent a text book example of a successive change in dominant exchange mechanism from (1) Ruderman–Kittel degenerate gas to (2) Baltensperger–de Graaf nondegenerate gas and finally to (3) Bloembergen–Rowland excitonic insulator. At very low temperatures, magnetic ordering is expected to break down because of the postulated weaker nature of exchange via excitonic states.

Yb(NH_3)$_6$ and Sr(NH_3)$_6$. Because the Yb^{2+} and Sr^{2+} cores are diamagnetic, it was expected that the molar susceptibilities of $Yb(NH_3)_6$ and $Sr(NH_3)_6$ would be about -60×10^{-6}, independent of temperature. Instead, it was found that the room-temperature values were about three times as great as this, and they crossed over to rather appreciable paramagnetic values at low temperatures. The predicted -60×10^{-6} value was calculated as the sum of the core diamagnetism (-15×10^{-6} for Sr^{2+} and -20×10^{-6} for Yb^{2+}, as given by Selwood (*17*)) plus the diamagnetism of the NH_3 (-16.3×10^{-6} emu per mole, as given for the gas by Angus (*18*)) plus the Pauli–Peierls conduction-electron spin susceptibility (about $+65 \times 10^{-6}$ emu per mole). The Pauli–Peierls susceptibility was calculated as elsewhere (*19*), assuming the effective mass to be equal to the electronic rest mass and taking two molecules of $M(NH_3)_6$ per unit cell of dimension 9.5×10^{-8} cm with two conduction electrons per molecule. It is probably not significant that the observed diamagnetism was more negative than expected. Not only were the measured forces extremely small, but there was uncertainty as to whether the diamagnetic correction for NH_3 should be taken to be that appropriate for a gas or the considerably more negative value appropriate for the solid. (Since solid NH_3 is hydrogen bonded, unlike $M(NH_3)_6$, it is not obvious that one should use the diamagnetic increment of solid NH_3 in our calculation.)

The low-temperature cross-over to paramagnetic behavior is believed to be real. As can be seen from the bottom of Table III, the low-temperature moment corresponds to a not-negligible value of 0.5 BM at liquid-helium temperature. (This moment was calculated as $\mu_{\text{eff}} = 2.8(\chi T)^{1/2}$ where χ is the observed molar susceptibility minus the diamagnetism of core ion and NH_3). It is not believed to stem from an impurity, since the $Yb(NH_3)_6$ and $Sr(NH_3)_6$ force curves crossed that of the sample holder in the same way, and there was no field-dependence of the susceptibility. It is believed, rather, that the cross-over to paramagnetism may reflect the same kind of conduction band collapse as postulated above for $Eu(NH_3)_6$ with onset of electron localization at 5*d*- (for Yb) or 4*d*- (for Sr) levels. Low-temperature electrical studies would be of interest.

Acknowledgment

We thank Professors W. E. Wallace and R. S. Craig of the University of Pittsburgh for making available the facilities of their well-equipped laboratory for some of the above measurements.

References

1. For a recent review of metal–ammonia research see the proceedings of the Lille conference in "Metal-Ammonia Solutions," (G. Lepoutre and M. J. Sienko, eds.). W. A. Benjamin, Inc., N.Y. 1964.

2. J. C. Warf and W. L. Korst, *J. Phys. Chem.* **60**, 1590 (1956).

3. H. J. Holland and F. W. Cagle, Jr., presented at the 145th National Meeting of the American Chemical Society, New York, N.Y. September 1963.

4. N. Mammano and M. J. Sienko, *J. Am. Chem. Soc.* **90**, 6322 (1968).

5. M. A. Ruderman and C. Kittel, *Phys. Rev.* **96**, 99 (1954).

6. R. A. Butera, R. S. Craig, and L. V. Cherry, *Rev. Sci. Inst.* **32**, 708 (1961).

7. W. T. Zachariasen, *in* "The Actinide Elements," (G. T. Seaborg and J. J. Katz, eds.), p. 775. McGraw-Hill, New York (1954).

8. See, for example, R. Catterall in Ref. 1, page 53.

9. American Chemical Society, "Thermodynamic Properties of the Elements," *Adv. Chem. Ser.* **18**, (1956).

10. Nat. Bur. Stand. (U.S.), "Selected Values of Chemical Thermodynamic Properties," Circ. 500, Wash. D.C., 1952.

11. L. V. Coulter, *J. Phys. Chem.* **57**, 553 (1953).

12. C. E. Moore, "Atomic Energy Levels as Derived from the Analyses of Optical Spectra, Circ. 467" (Nat. Bur. of Stand., Wash., D.C., 1949–1958); *J. Opt. Soc. Am.* **53**, 886 (1963).

13. See, for example, C. Kittel, "Quantum Theory of Solids," p. 88, Wiley, New York (1963).

14. P. K. Baltzer, P. J. Wojtowicz, M. Robbins, and E. Lopatin, *Phys. Rev.* **151**, 367 (1966).

15. W. Baltensperger and A. M. de Graaf, *Helv. Phys. Acta* **33**, 881 (1960).

16. N. B. Bloembergen and T. J. Rowland, *Phys. Rev.* **97**, 1679 (1955).

17. P. W. Selwood, "Magnetochemistry," 2nd Ed., p. 78. Interscience, New York (1956).

18. W. R. Angus in Landolt-Bornstein "Zahlenwerte und Funktionen," Vol. II, Part 10, Magnetic Properties II, p. 34. Springer-Verlag, Berlin (1967).

19. M. J. Sienko, *Adv. Chem. Ser.* **39**, 231 (1963).